Foam-like 3-D graphene coatings for cooling systems involving phase change

Abdolali K Sadaghiani[Θ], Ahmad Reza Motezakker[Θ], Sibel Kasap[§], Ismet I Kaya [Θ,§], Ali Koşar[§,Θ,,¥].*

[*] Faculty of Engineering and Natural Sciences, Sabanci University, Tuzla, 34956, Istanbul, Turkey

[§] Sabanci University Nanotechnology and Application Center (SUNUM), Sabanci University, Tuzla, 34956, Istanbul, Turkey

[¥] Center of Excellence for Functional Surfaces and Interfaces for Nanodiagnostics (EFSUN), Sabanci University, Tuzla, 34956, Istanbul, Turkey

[*] Corresponding author

Supplementary Note 1.

Preparing 3-D foam-like graphene coating by Chemical Vapor Deposition method (CVD)

After the foams were cut to a size of 10mm×10mm, they were placed in the central zone of a horizontal quartz tube of a length of 1400 mm. Prior to the experiments, the vacuum chamber was evacuated using a dry pump until the pressure reached 2×10^{-2} Torr. Then, the furnace was heated up to the desired growth temperature within 20 min under H_2 and Ar flows. To provide a homogeneous graphene coating on a nickel foam substrate, the foams were annealed for 10 min with Ar and H_2 gases at the growth temperature. CH_4 as a carbon precursor was propelled at the required flow rate into the quartz tube for 7.5 to 12 min for the growth of graphene foams. Finally, the samples were allowed to cool down to the ambient temperature under Ar flow. The CVD growth conditions are summarized in **Table S.1**.

Table S1. Growth parameters for prepared graphene foams using the chemical vapor deposition (CVD) method.

Sample No	Growth Temperature (°C)	Growth time (min.)	CH_4 (sccm)	H_2 (sccm)	Ar (sccm)
#1	975	12.5	80	100	275
#2	975	12.5	80	100	425
#3	975	7.5	80	100	275
#4	925	7.5	80	100	275

In this study, three-dimensional graphene foams are transferred on SiO_2 surfaces using the wet etching procedure. The detailed transfer procedure is given in **Figure S1**.

Figure S1. Transfer of graphene foam on substrates.

SiO_2 surfaces contain abundant silanol (SiOH) groups. These groups are sensitive to the adsorption of water molecules. SiO_2 surface is therefore hydrophilic. On the other hand, graphene exhibits a hydrophobic characteristic. This hydrophilic/hydrophobic interaction causes instability in the interface between graphene and SiO_2 during transfer of graphene via the wet etching procedure [1-5].

As a result, graphene does not attach to SiO_2 surface properly. In this study, the adhesion between foam and substrate was optimized using the heating procedure. First, samples (GF/substrate) were heated at different temperatures such as 25°, 40° and 80° and then were immersed into water. The immersion tests of samples into water are included in **Figure S2**. As seen in **Figure S2(a)** and **Figure S2(b)**, foams heated at 25° and 40° separated from the substrate when they were immersed into water. On the other hand, the foam heated at 80° did not separate from the substrate when it was immersed into water (**Figure S2(c)-Figure S2(d)**).
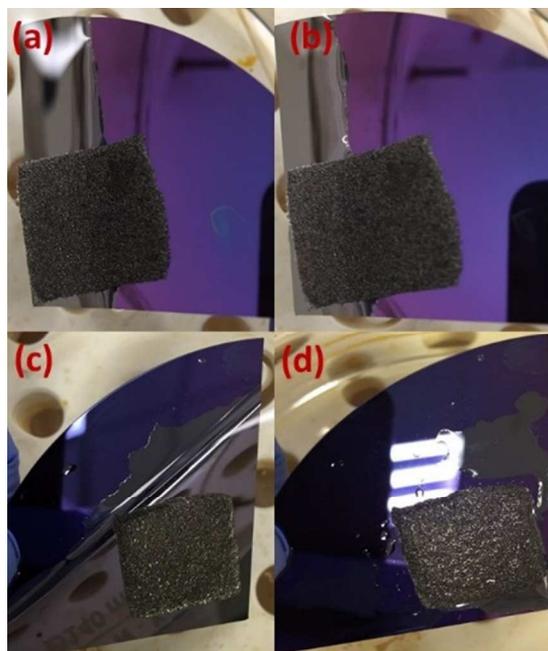
Figure S2. Adhesion tests between graphene foam and substrate

A sample fabrication is detailed in **Figure S3a**. In addition, the transfer procedure is given in **Figure S3b**.
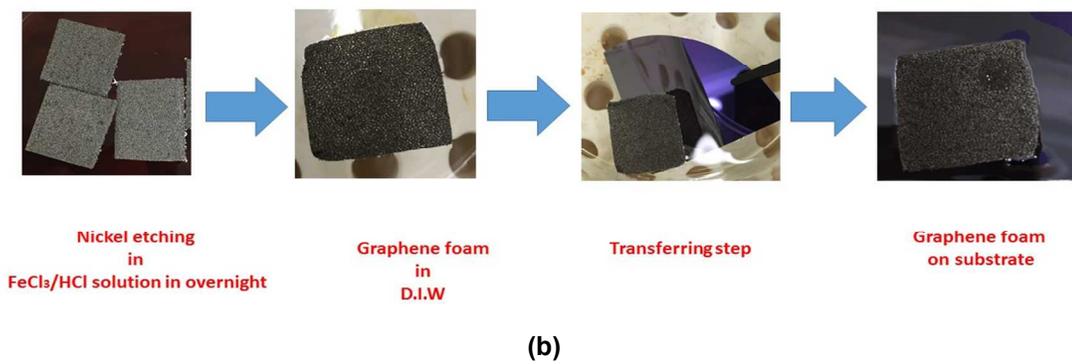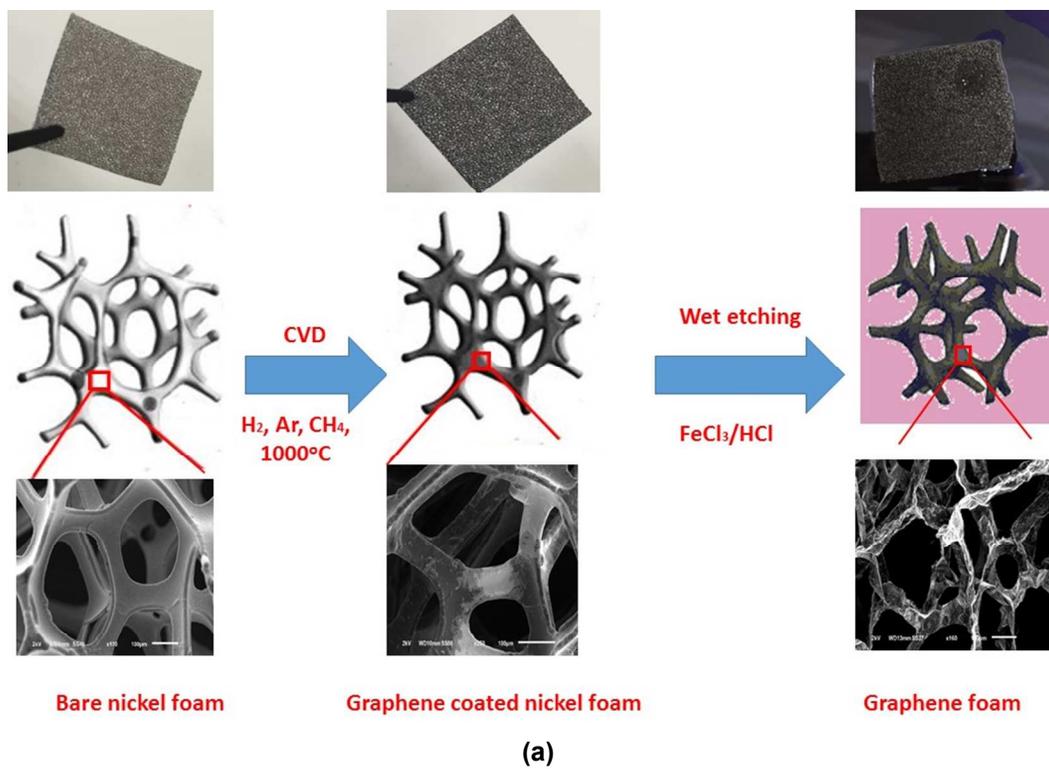
(a)

(b)

Figure S3. (a) Fabrication of graphene foam by CVD method, (b) Transfer procedure of graphene foam.

Supplementary Note 2.

XRD spectrum and SEM images of the 3D graphene foam

Figure S4a displays XRD spectrum of the 3D graphene foam (sample #4). The sharp diffraction peaks (2θ) at 26.5°, corresponding to the plane (002), are reflections of the high crystallinity of defect-free CVD grown graphene. (JCPDS 75-1621). In **Figure S4b**, Raman spectrum of the 3D-graphene foam (Sample-4) is depicted. In this spectrum, three specified graphene peaks centered at 1580, 2550 and 2720 cm^{-1}, which are attributed to G, G* and 2D bands as can be clearly observed, while the D band at 1350 cm^{-1} (which is associated with disorders) cannot be detected. The absence of D peak in Raman spectrum indicates that graphene foams are of high quality. The intensity of I2D/IG correlated with number of graphene layers was calculated sd between 1.58 and 0.36 for graphene foams. According to this result, it can be deduced that single-layer and multi-layer graphene flakes coexist together in 3D-graphene foams.
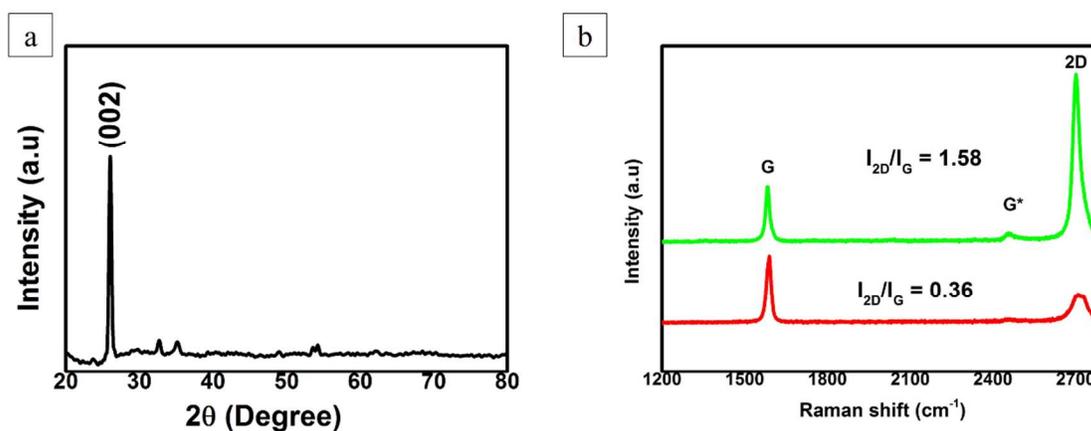

Figure S4. a) XRD spectrum of 3D-graphene foam (samle-4) b) Raman spectrum of 3D-graphene foam (sample-4)

Figure S5 shows the SEM images of graphene coatings with different surface areas. The Network density and pore size distributions are seen in SEM images.
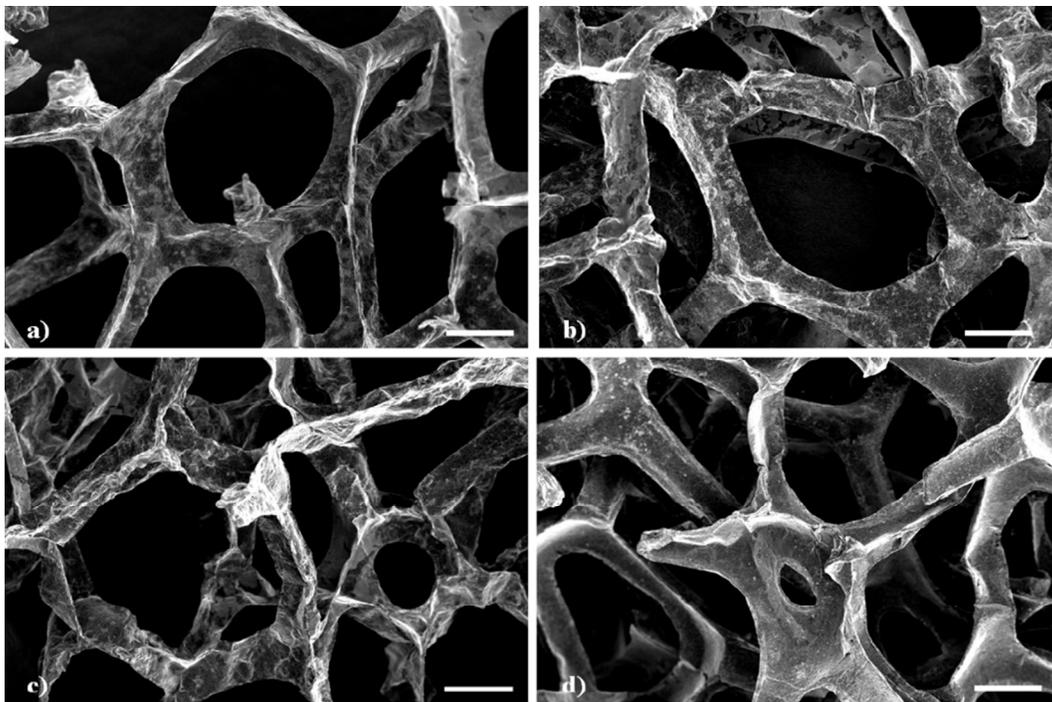
Figure S5. SEM images of a) 8nm b) 13nm c) 29nm d) 55nm, 3-D foam-like graphene structure

Supplementary Note 3

Experimental setup and procedure details

Pool boiling experiments were conducted under atmospheric pressure using deionized water as the working fluid. The schematic of the experimental setup consisting of holders, a heater block, a glass block for visualization, six thermocouples, four cartridge heaters, gasket sealers and a vertical reflux condenser is shown in **Figure S6**. All of the samples have an area of 4×4 cm^2 and are attached on top of the aluminum block surface with dimensions of 6×6 cm^2. A glass hollow cube with the outer and inner dimensions of 6×6×6 cm^3, and 4×4×6 cm^3, respectively, were attached on top of the sample and heating block.
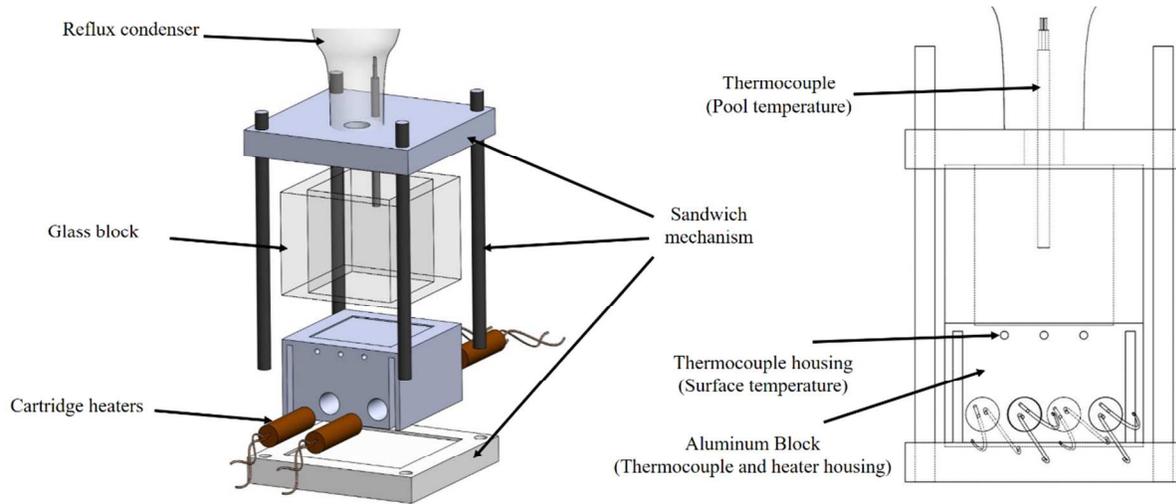

Figure S6. Schematic of the pool boiling experimental setup.

To calculate the net heat flux value applied from the bottom wall, the below equation was used:

$$q'' = \frac{VI - Q_{loss}}{A}$$

(S.1)

where, V is the applied voltage, I is the current, A is the heated surface area. To calculate the heat loss, Q_{loss}, a natural convection analysis for areas of the heater, which were in contact with the environment, was performed. According to the analysis, the heat losses were between 2% and 4.5%. The boiling heat transfer coefficient, h, was calculated as:

$$h = \frac{q''}{T_w - T_f} \tag{S.2}$$

Here, T_W is the wall temperature, and T_f is the fluid bulk temperature. For subcooled boiling, T_f was measured using a T-type thermocouple, while for saturated boiling the fluid temperature was taken as saturation temperature. Wall superheat, ΔT_{sat}, is defined as the difference between the saturation temperature, T_{sat}, and the average surface temperature, T_s. The wall temperatures were obtained by considering the thermal contact resistance from the thermocouple to the surface R_C and the average of the thermocouple measurements T_{th}, as:

$$T_s = T_{th} - q'' \times R_c \tag{S.3}$$

In the light of the datasheet of the thermal paste, its contact resistance was taken as 6×10^{-6} (m^2K/W).

To find the uncertainties in experimental parameters, an uncertainty analysis was performed according to the method proposed by Coleman and Steel [6], and the uncertainties are shown in Table 3.

Table S2. Estimated uncertainties of experimental parameters

Parameter	Uncertainty	Parameter	Uncertainty
Electrical Power	±1.3%	Fluid Temperature	±5-8%
Wall Temperature	±1-7%	Heat Transfer Coefficient	±5-10%
Area	±1-7%	Heat Flux	±2-6%

To minimize the amount of heat losses, the aluminium heating part was fitted into a Teflon block acting as an insulator. To calculate the amount of heat loss for each experiment, a natural convection heat transfer analysis was performed. Accordingly, the range of ratio of heat loss to the input power was found as 2% to 4.5%.

Supplementary Note 4

Force expressions

The expressions for the mentioned forces are as follows:

Bubble growth $\qquad F_{growth} = 10\, \rho_l \pi\, \dot{D}^2 D^2$ $\hspace{5cm}$ (S.4)

Buoyancy $\qquad F_{Buo} = \left(\rho_l - \rho_g \right) g \left[\frac{\pi}{3} \left(\frac{D^3}{4} + \frac{D^2}{4} \sqrt{D^2 - D_p^2} + \frac{D_p^2}{8} \sqrt{D^2 - D_p^2} \right) \right]$ $\hspace{1cm}$ (S.5)

Surface tension $\qquad F_{ST} = \sigma\, \pi\, D_p \sin\left(\sin^{-1}\left(\frac{D_p}{D} \right) \right)$ $\hspace{3cm}$ (S.6)

Lift force $\qquad F_{Lift} = \frac{2.4}{8} \pi\, \rho_l \left(D_b\, \dot{D} \right)^2$ $\hspace{5cm}$ (S.7)

Inertia force $\qquad F_{Inertia} = \dot{D}^2\, \rho_v\, \frac{\pi}{12} \left(\frac{3D^2}{4} + \frac{1}{4} \left(\frac{D^3 - 2DD_p^2}{\sqrt{D^2 - D_p^2}} \right) - \frac{D_p^2 D}{8\sqrt{D^2 - D_p^2}} \right)$ $\hspace{1cm}$ (S.8)

Here, ρ, D, D_d, and σ are density, bubble diameter, and bubble departure diameter, respectively [7-8]. The departure diameter can be obtained at the departure time by balancing the acting forces on the bubble.
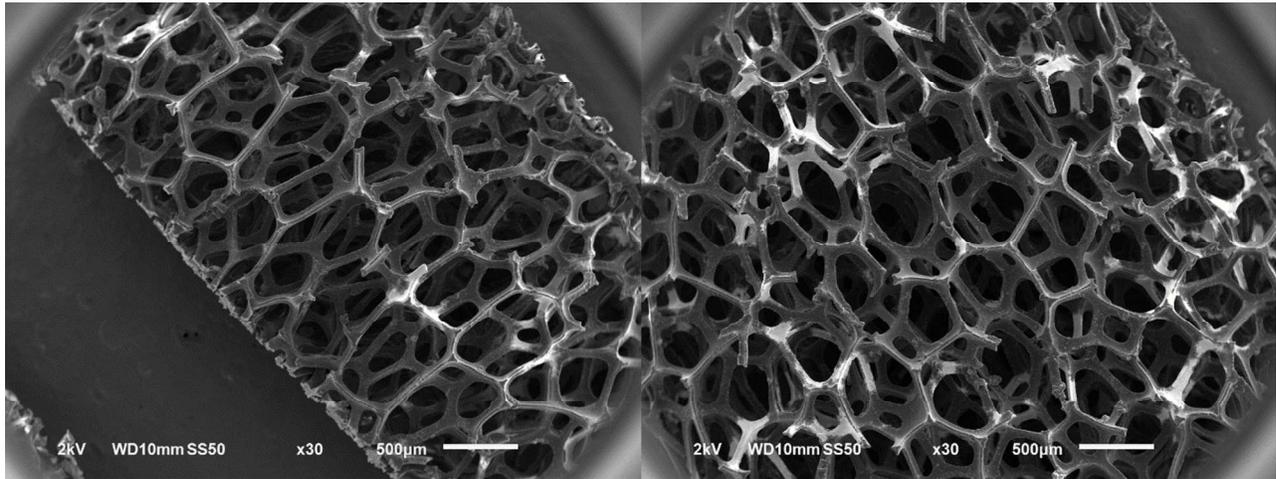
Supplementary Note 5

SEM images of graphene coated Ni foams is shown in **Figure S7**. The white areas indicate the regions where the graphene is not coated. As seen, the density of white areas increases as graphene thickness decreases.

Sample #1   **Sample #2**

Sample #3   **Sample #4**

Figure S7. SEM images of different samples indicating uncoated graphene areas on Ni foam

Figure S8 shows the uncoated graphene rods for 3DG foam with 13nm graphene thickness. The image indicates that the disconnectivity in the branches increases the pore size, which dramatically affect the boiling process in developed nucleate boiling region.
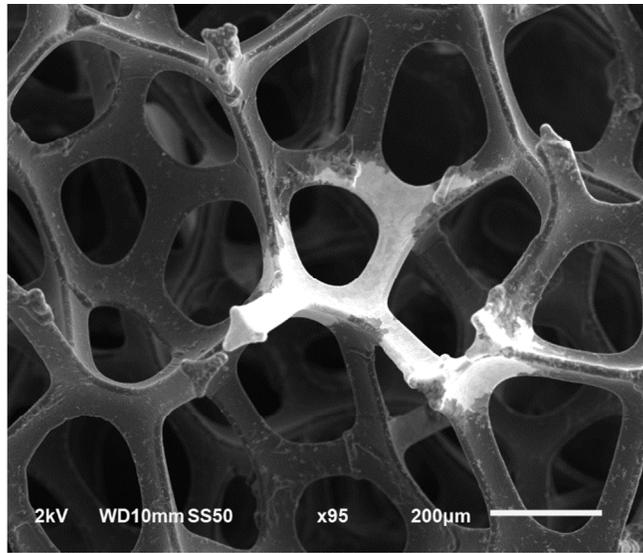
Figure S8. SEM image of uncoated area on Sample #1

Supplementary Note 6

The effect of graphene coating on bubble departure process is shown in **Figure S9**. At high heat fluxes, the graphene coating raises the bubble departure frequency. Smaller bubbles depart from the surface, while higher concentration of coalesced bubbles is visible.
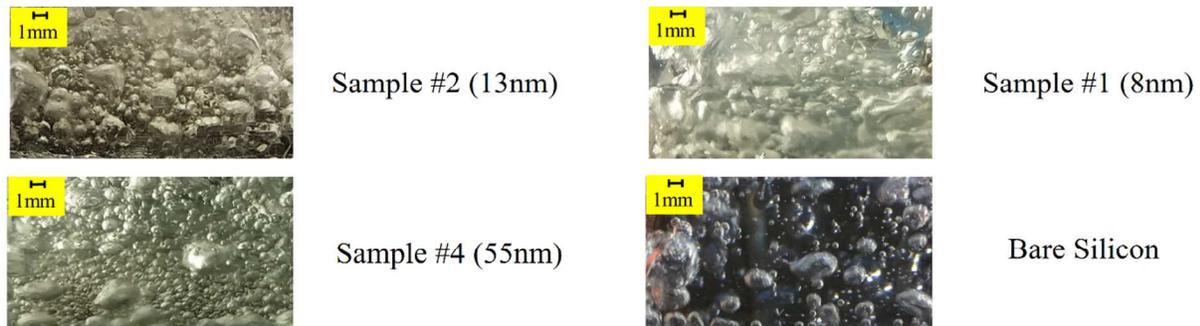

Figure S9 Generated bubbles for different coatings and bare silicon surfaces at the heat flux of 90 kW/m^2.

References:

(1) Gao, W.; Liechti, K. M.; Huang, R., Wet adhesion of graphene. *Extreme Mechanics Letters* **2015,** *3*, 130-140.

(2) Asay, D. B.; Kim, S. H., Evolution of the adsorbed water layer structure on silicon oxide at room temperature. *The Journal of Physical Chemistry B* **2005,** *109 (35)*, 16760-16763.

(3) Gao, L.; Ni, G.-X.; Liu, Y.; Liu, B.; Neto, A. H. C.; Loh, K. P., Face-to-face transfer of wafer-scale graphene films. *Nature* **2014,** *505 (7482)*, 190.

(4) Lee, M. J.; Choi, J. S.; Kim, J.-S.; Byun, I.-S.; Lee, D. H.; Ryu, S.; Lee, C.; Park, B. H., Characteristics and effects of diffused water between graphene and a SiO 2 substrate. *Nano Research* **2012,** *5 (10)*, 710-717.

(5) Kumar, S.; Parks, D.; Kamrin, K., Mechanistic origin of the ultrastrong adhesion between graphene and a-SiO2: beyond van der Waals. *ACS nano* **2016,** *10 (7)*, 6552-6562.

(6) Coleman, H. W.; Steele, W. G., *Experimentation, validation, and uncertainty analysis for engineers*. John Wiley & Sons: 2009.

(7) Ramaswamy, C.; Joshi, Y.; Nakayama, W.; Johnson, W., Semi-analytical model for boiling from enhanced structures. *International Journal of Heat and Mass Transfer* **2003,** *46 (22)*, 4257-4269.

(8) Zeng, L.; Klausner, J.; Mei, R., A unified model for the prediction of bubble detachment diameters in boiling systems—I. Pool boiling. *International Journal of Heat and Mass Transfer* **1993,** *36 (9)*, 2261-2270.